Published online 26 July 2023

Nucleic Acids Research, 2023, Vol. 51, No. 17 ***9385–9396***
https://doi.org/10.1093/nar/gkad619

CSDE1 promotes miR-451 biogenesis

Pavan Kumar Kakumani [1,*], Yunkoo Ko[2], Sushmitha Ramakrishna[1], Grace Christopher[1], Maria Dodgson[1], Jatin Shrinet[3], Louis-Mathieu Harvey[4,5], Chanseok Shin[2,6,7] and Martin J. Simard[4,5,*]

[1]Department of Biochemistry, Memorial University of Newfoundland, 45 Arctic Avenue, St. John's NL A1C 5S7, Canada, [2]Department of Agricultural Biotechnology, Seoul National University, Seoul 08826, Republic of Korea, [3]Department of Biological Science, Florida State University, 319 Stadium Drive, Tallahassee, FL 32306-4295, USA, [4]Oncology Division, Centre Hospitalier Universitaire de Québec-Université Laval Research Center (L'Hôtel-Dieu de Québec), Quebec City, Québec G1R 3S3, Canada, [5]Laval University Cancer Research Centre, Québec City, Québec G1R 3S3, Canada, [6]Research Center for Plant Plasticity, Seoul National University, Seoul 08826, Republic of Korea and [7]Research Institute of Agriculture and Life Sciences, and Plant Genomics and Breeding Institute, Seoul National University, Seoul 08826, Republic of Korea

Received August 19, 2022; Revised July 06, 2023; Editorial Decision July 07, 2023; Accepted July 14, 2023

ABSTRACT

MicroRNAs are sequentially processed by RNase III enzymes Drosha and Dicer. miR-451 is a highly conserved miRNA in vertebrates which bypasses Dicer processing and instead relies on AGO2 for its maturation. miR-451 is highly expressed in erythrocytes and regulates the differentiation of erythroblasts into mature red blood cells. However, the mechanistic details underlying miR-451 biogenesis in erythrocytes remains obscure. Here, we report that the RNA binding protein CSDE1 which is required for the development of erythroblasts into erythrocytes, controls the expression of miR-451 in erythroleukemia cells. CSDE1 binds miR-451 and regulates AGO2 processing of pre-miR-451 through its N-terminal domains. CSDE1 further interacts with PARN and promotes the trimming of intermediate miR-451 to the mature length. Together, our results demonstrate that CSDE1 promotes biogenesis of miR-451 in erythroid progenitors.

GRAPHICAL ABSTRACT

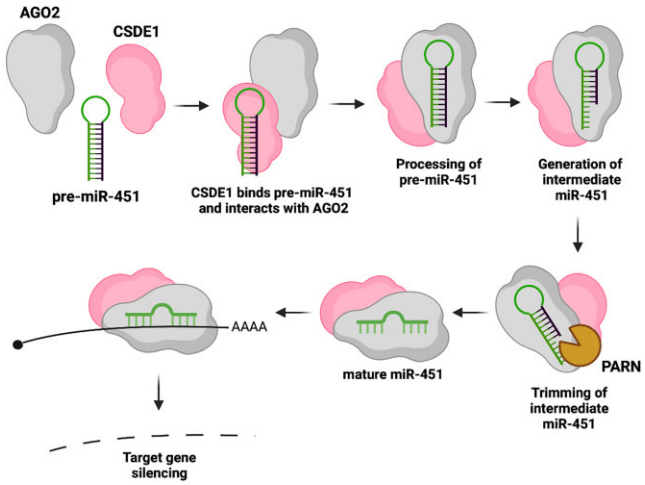

INTRODUCTION

In the microRNA (miRNA) pathway, canonical miRNAs undergo sequential cleavage by the ribonuclease III enzymes, Drosha and Dicer (1) which process primary miRNAs (pri-miRNAs) into precursor miRNAs (pre-miRNAs) and eventually into mature miRNAs of length 21–23 nucleotides (nt), respectively. These duplex miRNAs are then loaded onto Argonaute (AGO) proteins to mediate translational repression of target mRNAs coupled with de-adenylation and decay (2). However, several miRNAs have been evolved to circumvent processing by Drosha-DGCR8 protein complex in the nucleus. For instance, mirtrons are derived from intronic regions (3–5) and the

*To whom correspondence should be addressed. Tel: +1 709 864 2501; Email: pavan.kakumani@mun.ca
Correspondence may also be addressed to Martin J. Simard. Tel: +1 418 525 4444; Email: Martin.Simard@crchudequebec.ulaval.ca

corresponding splice sites define the ends of their precursor miRNAs. Pre-miRNAs also arise from tRNA genes, where the 5′ end is defined by RNaseZ cleavage and the 3′ end corresponds to transcription termination by RNA polymerase III (6). Other Drosha-independent miRNAs are generated from certain small nucleolar RNAs (snoRNAs) or directly from the 5′ end of Pol II transcribed genes (7,8). In contrast to these non-canonical miRNAs, miR-451, a vertebrate specific miRNA, is the only known example of a miRNA whose biogenesis is strictly independent of Dicer. miR-451 is transcribed together with miR-144 from a bicistronic locus and processed by Drosha into an unusually short, 41 to 42 nt pre- miR-451 hairpin with a highly structured 17 nt stem region and 4 nt terminal loop. Pre-miR-451 is too short to be cleaved by Dicer and is directly loaded into AGO2 protein. Unlike canonical miRNAs, maturation of miR-451 requires the slicer activity of AGO2 (9–12). In zebrafish, mice and humans, AGO2 cleaves the 3′ arm of pre-miR-451 through its slicer activity and yields a 30 nt intermediate RNA which undergoes 3′ to 5′ trimming mediated by poly(A)-specific ribonuclease (PARN) to generate mature miR-451 (13).

miR-451 is the most abundant miRNA in mature erythrocytes and the AGO2-dependent processing of miR-451 in erythropoiesis is conserved across all vertebrates (14–17). The loss of function of miR-451 in zebrafish and mice leads to incomplete erythrocyte differentiation and increased susceptibility to oxidative stress, whereas the gain of function of miR-451 is associated with the blood cancer, polycythemia vera. miR-451 expression is linked to acute and chronic myeloid leukemias in which the process of erythroblast differentiation into mature red blood cells becomes subverted (14,15,18–21). miR-451 is refractory to the global downregulation of canonical miRNAs triggered by negative feedback loop between miR-144 and Dicer during erythropoiesis (22). Yet, there is no direct evidence on cellular factors that govern cell specific expression of miR-451 and promote AGO2-dependent processing of miR-451 during hematopoiesis, especially in erythrocytes.

CSDE1, also known as UNR (upstream of N-Ras), is a member of the evolutionarily conserved CSD (cold shock domain) containing protein family (23). CSDE1 contains at least 5 CSDs and is known to regulate translation and mRNA stability in various organisms (24). In *Drosophila melanogaster*, this protein is part of a translational repressor complex assembled at the 3′ UTR of *male-specific lethal-2* (msl-2) mRNA and is critical for the proper regulation of X-chromosome dosage compensation (25,26). In mammalian cells, CSDE1 binds to its own IRES (internal ribosome entry site) to repress translation but can also enhance IRES-dependent translation of select mRNAs, such as Apaf1 and Cdk11B, in co-operation with nPTB and hnRNPC1/C2, respectively (27–30). CSDE1 was also shown to interact with PABP to control the stability of c-fos mRNA, and with AUF1 to regulate that of PTH mRNA (31). Further, CSDE1 regulates the stability and translation of FABP7 and VIM mRNAs in human Embryonic Stem Cells while it controls GATA6 post-transcriptionally in mouse Embryonic Stem Cells (32,33). Interestingly, in melanoma, CSDE1 regulates the levels of transcripts encoding oncogenes and tumor suppressors and promotes the translation elongation of critical epithelial-to-mesenchymal transition (EMT) markers, namely Vimentin (VIM) and RAC1, to enhance invasion and metastasis both *in vitro* and *in vivo* (34). We have recently shown that CSDE1 interacts with the miRISC, especially AGO2 in *Drosophila* embryo extracts, mouse and human cell lines and further associates with DCP1-DCP2 decapping complex to render target mRNAs susceptible to miRNA-guided gene silencing (35). Further, CSDE1 interaction with AGO2 is partially dependent on target mRNAs in melanoma cells, and binding to its signature motifs on 3′ UTR of mRNAs counters AGO2/miRNA-guided translational repression, especially of PMEPA1 to promote melanoma tumorigenesis (36). Besides, CSDE1 is highly expressed in myeloid lineage and critical for proliferation as well as differentiation of erythroblasts into mature red blood cells (37). However, the mechanisms underlying its role in erythropoiesis are unknown.

In the present study, we investigated the regulatory role of CSDE1 in miRNA expression underlying the development of red blood cells. Here, we used small RNA libraries from CSDE1 KO cell lines and discovered that CSDE1 effects miR-451 expression in erythroid progenitors. Analysis of miR-451 expression at both precursor and mature levels show that CSDE1 controls the processing of pre-miR-451 and trimming of intermediate miR-451 in association with AGO2 and PARN, respectively. Together, our findings reveal a unique role for CSDE1 in the biogenesis of erythrocyte specific miR-451.

MATERIALS AND METHODS

Cell culture and transfection

HEK293T and MEL cells were grown in Dulbecco's modified Eagle's medium (DMEM) and Roswell Park Memorial Institute (RPMI) 1640 Medium respectively supplemented with 10% fetal bovine serum, 50 U/ml penicillin, and 50 μg/ml streptomycin. The transfections in HEK293T cells were performed using jetPRIME reagent following the manufacturer's instructions (Polyplus transfection SA, Illkirch, France).

Generation of CSDE1 KO HEK293T cells

CRISPR/Cas9-mediated gene knockout (KO) was performed as described previously (38). In briefly, *CSDE1* knockout cell line was generated by using CRISPR/CAS9 system vector pSpCas9(BB)-2A-Puro (Addgene, ID: 48139) containing a single guide RNA targeting the human *CSDE1* gene in HEK293T cells. Knockout single cell colonies were isolated and screened for the absence of CSDE1 protein by western blotting and PCR-based genotyping to check frame shifting mutation.

In vitro trimming assays

HECK293T WT or *CSDE1* KO lysate with transiently expressed FLAG-hAGO2 was used for *in vitro* trimming assays. (38,39). *In vitro* trimming assay was performed with some modifications from the previously described method (38). In briefly, 2.5 μl of cytoplasmic lysate, 1.5 μl reaction buffers, and 0.5 μl of 200 nM radiolabeled ac-pre-miR-451s

were used in the assay. Reaction samples were first incubated at 25°C for 30 min and incubated at 37°C for the indicated time periods. The reactions were stop by quenching with 2X formamide dye followed by heating at 95°C for 5 min. The products were then resolved on 15% urea-polyacrylamide gel. The separated bands were detected by Typhoon FLA-7000 image analyzer (Fujifilm Life Sciences) and quantified by ImageJ software.

Plasmids

pCDNA6.2-hsa-miR-144/451 and miR-451 sensor in psiCHECK2 were a kind gift from Eric Lai, Memorial Sloan Kettering Cancer Center, USA (40). The mutations in CSD binding motif on miR-451 sequence were generated using Q5 Site-Directed Mutagenesis Kit as per manufacturer instructions (NEB). Plasmids expressing FLAG-CSDE1 or deletion mutants and myc-PARN were described previously (35,38). The FLAG/HA-AGO2 was received from Dr Gunter Meister, University of Regensburg, Germany.

Antibodies

Antibodies against CSDE1 (ab201688), AGO2 (ab57113, ab186733) and β-actin (ab49900) are from Abcam. FLAG (F1804-200UG), STRAP (NBP2-24740SS) antibodies are from Sigma-Aldrich, Oakville, Ontario and Novus Biologicals respectively. The AGO2 antibody (11A9) was received from Dr Gunter Meister laboratory, University of Regensburg, Germany. Antibodies against HA (3724S) and GATA2 (4595S) were purchased from Cell Signaling Technology, Massachusetts, USA. c-Myc antibody (9E10) (13-2500) and PARN antibody (A303-562A-T) were procured from Thermofisher and Bethyl Laboratories Inc., respectively.

Small RNA library preparation and computational analysis of sequencing reads

Total RNAs from the Control and CSDE1 KO MEL cells were used to construct small RNA libraries that consists of RNAs at ∼20–30 nt in length, as described previously (41). The small RNA libraries have undergone high throughput sequencing and the sequence reads were subjected to quality check using FastQC tool (http://www.bioinformatics.babraham.ac.uk/projects/fastqc/) as described previously (42). Further the reads were subjected to trimming and adaptors were removed using TrimGalore tool (43). Mouse miRNA sequences (mature and precursor) were downloaded from miRBase (v. 22) (44–45) database and the filtered reads from each replicate were matched to the known mouse mature miRNA and precursor miRNA sequences separately using Bowtie tool (46). The reads aligned to precursor miRNAs were used to count the isomiRs. The read counts were then normalized, and Transcript per Kilo Base per Million (TPM) values were calculated, and sequence lengths were obtained for each isomiRs.

Co-immunoprecipitation

Cells were homogenized in the lysis buffer with protease and phosphatase inhibitor cocktail. The lysate was centrifuged at 15 000g for 15 min, the supernatant was collected and measured for protein concentration using Bradford reagent. Meanwhile, Dynabeads Protein G (Thermofisher) were prepared in an Eppendorf (25 μl for a total protein extract of 2 mg and 10 μg of antibody). The beads were washed with 3 times the volume of lysis buffer and was repeated two more times. The lysate was preincubated with the equivalent of Dynabeads at 4°C on a nutator for about 45 min. The lysate was collected, and the respective antibody added to incubate on nutator at 4°C for overnight. The next day, Dynabeads were prepared (as stated previously), and the lysate was added to incubate on the rotator at room temperature for about 90 min. For RNase treatment, the RNases A&T1 were added at a concentration of 4 μg and 1 unit respectively per 1 mg of total protein extract in buffered solution to the beads and incubated at RT for 15 min. The beads were washed about 5 times with lysis buffer and the samples were extracted for western blotting by adding SDS loading buffer in 1× concentration and heating at 100°C. For Northern blotting, the samples were extracted using Trizol as per manufacturer's instructions (Thermofisher).

Northern blotting

Total or immunoprecipitated (IP'ed) RNAs were separated on 15–20% PAGE-8M Urea gels, transferred onto a Genescreen plus membrane (Perkin-Elmer) and crosslinked using 1-ethyl-3-(3-dimethylaminopropyl) carbodiimide hydrochloride (EDC) (Sigma) as described in (47). DNA probes radiolabeled with the Starfire system (IDT) were hybridized to the membrane. After washing, the membrane was exposed to an image plate and scanned with the FLA-5100 phospho-imager. The oligonucleotide probes (the GGCGGG sequence at the 3′ end is the adaptor for binding to the extension template oligonucleotide) are listed as follows:

miR-451: 5′-AACTCAGTAATGGTAACGGTTT GGC GGG-3′

miR-144–3p: 5′-AGTACATCATCTATACTGTA GGC GGG-3′

miR-21–5p: 5′-TCAACATCAGTCTGATAAGCTA G GCGGG-3′

miR-362–5p: 5′-ACTCACACCTAGGTTCCAAGGAT T GGCGGG-3′

U6 snRNA: 5′-GCAGGGGCCATGCTAATCTTCTC TGTA GGCGGG-3′

let-7: 5′-AACTATACAACCTACTACCTCA GGCGG G-3′

Statistical analysis

Data are presented as mean ± SD and the results were compared using two-tailed Student's *t*-test. *P*-value <0.05 was considered statistically significant. Sample size (*n*, biological replicates) and *P*-values are shown in the figure legends and significance was considered as $*P < 0.05$; $**P < 0.03$; $***P < 0.01$; n.s., not significant.

RESULTS

CSDE1 controls the expression of erythroid specific miR-451

To investigate the regulatory role of CSDE1 in miRNA expression, we sequenced small RNA libraries from Control

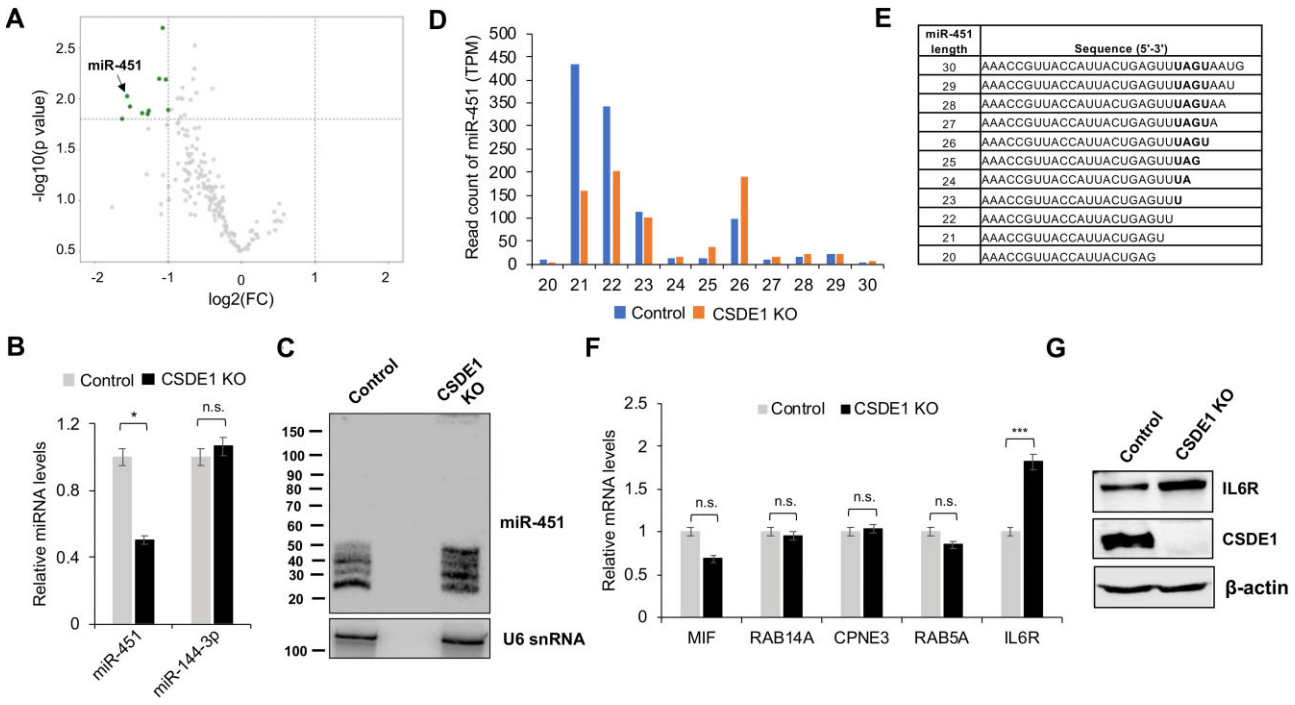

Figure 1. CSDE1 loss downregulates miR-451 expression at post-transcriptional level. (**A**) Volcano plot representing miRNA differential expression analysis of small RNA libraries prepared from total RNA of Control and CSDE1 KO murine erythroleukemia (MEL) cells. (**B**) Relative miRNA levels of miR-451, miR-144-3p in total RNA from Control and CSDE1 KO MEL cells. Data are presented as mean ± SD (*$P < 0.05$, $n = 3$, two-tailed t test). Trizol extraction method was used to isolate the RNA and RT-qPCR was performed to quantify miRNA levels. (**C**) Expression analysis of miR-451 measured by northern blotting of total RNA from Control and CSDE1 KO MEL cells. (**D**) Bar graph representing read count for relative length distribution of miR-451 from Control and CSDE1 KO MEL cells. E) Representative miR-451 read sequences observed in small RNA libraries. F) Relative mRNA levels of miR-451 targets in total RNA from Control and CSDE1 KO MEL cells. Data are presented as mean ± SD (***$P < 0.01$, $n = 3$, two-tailed t test). Trizol extraction method was used to isolate the RNA and RT-qPCR was performed to quantify the mRNA levels. (**G**) Western blot confirming the expression of proteins indicated in Control and CSDE1 KO MEL cells. β-actin was used as a loading control.

and CSDE1 knock out (KO) erythroid cells. The CSDE1 KO MEL cells were generated using CRISPR/Cas9, and they were a generous gift from Prof. Marieke von Lindern (48). Our miRNA differential expression analysis revealed that miR-451 is significantly downregulated in CSDE1 KO cells relative to the Control cells (Figure 1A, Supplemental File 1). Also, we observed downregulation in the expression of some of the known canonical miRNAs from the RNA seq data, namely, miR-449a-5p, miR-497a-5p, miR-19b-1-5p, miR-708–5p, miR-200a-3p, miR-200b-3p, miR-30c-5p, miR-92b-3p, let-7f-1–3p, miR-17–5p, miR-20a-5p in CSDE1 KO cells. However, we observed no sequence correlation between primary transcripts of these miRNAs, suggesting indirect effects on their mature miRNA expression observed from RNA seq data analysis, in the absence of CSDE1 (Supplementary Figure S1). Since CSDE1 interacts with AGO2 (35) and miR-451 follows the non-canonical route (AGO2-dependent) for its biogenesis in erythroid cells, unlike the canonical miRNAs that are altered in CSDE1 KO cells, we focused on miR-451 and its relationship with CSDE1. We validated the changes in miR-451 expression under the Control and CSDE1 KO conditions, while there was no difference observed in miR-144-3p levels (Figure 1B), the canonical miRNA in miR-144/451 cluster specific to the haematopoietic system. We further confirmed the reduced expression of mature miR-451 in the case of CSDE1 KO MEL cells and interestingly, we observed an increase in the levels of processing intermediates of miR-451 which indicate that the effects of CSDE1 over miR-451 levels are at the post-transcriptional level (Figure 1C). Following, we examined miR-451 read sequences and their length distribution in the Control and CSDE1 KO libraries and observed that sequence reads outside the lengths of 20–30nt showed negligible read counts (Supplemental File 2). The normalized read count of miR-451 at 21 and 22 nt is reduced while there was an accumulation of longer reads (processing intermediates) at 26 nt under CSDE1 KO conditions relative to the Control cells (Figure 1D, Supplemental File 3) and a representative miR-451 sequence for each of the lengths between 20nt and 30nt is presented in Figure 1E. We observed no such variations in the distribution of sequence reads (mature vs possible precursor forms) of canonical miRNAs that showed reduced expression in CSDE1 KO cells, such as miR-708-5p, miR-19b-1-5p and miR-220a-3p, among others (Supplementary Figure S2). Simultaneously, we assessed for possible variations of miR-451 sequence reads from the data and observed that the positioning of nucleotide changes is mostly internal to the sequence (Supplemental file 2), thus supporting the comprehensive nature of our length distribution analysis and the absence of non-templated nucleotide additions to the miR-451 species in MEL cells. Furthermore, we examined the expression levels of valid miR-451 targets (MIF, RAB14A, CPNE2, RAB5A, IL6R (49)) and observed that the levels of IL6R

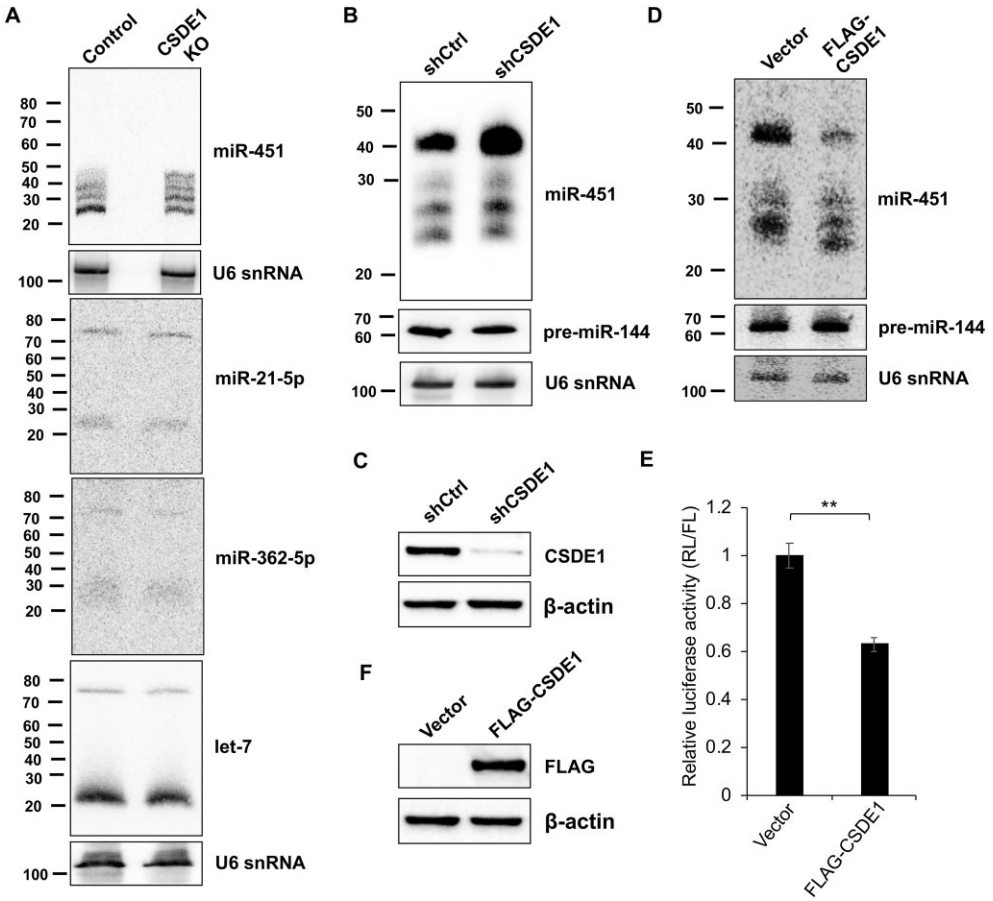

Figure 2. CSDE1 regulates the processing of miR-451**.** (**A**) Expression analysis of indicated miRNAs measured by northern blotting of total RNA from Control and CSDE1 KO MEL cells. (**B**) miR-451 expression measured by northern blotting of total RNA from Control and CSDE1 knockdown (shCSDE1) HEK293T cells transiently expressing miR-144/451 operon. The RNA extracts were run on the 8M urea–PAGE gel, and the miRNAs indicated were probed. Migration of the molecular weight marker is indicated (nt). Pre-miR-144 was probed as a transfection control while U6 snRNA was used as a loading control. (**C**) Western blots confirming the depletion of CSDE1 in shCSDE1 HEK293T cells. (**D**) Northern blot of miR-451 expression from total RNA of CSDE1 knockdown (shCSDE1) HEK293T cells transiently expressing miR-144/451 operon along with FLAG-tagged full length CSDE1. The samples were run on the 8 M urea–PAGE gel, and the miRNAs indicated were probed. Migration of the molecular weight marker is indicated (nt). Pre-miR-144 was probed as a transfection control while U6 snRNA was used as a loading control. (**E**) Relative luciferase expression (renilla/ firefly) of miR-451 reporter construct in CSDE1 knockdown (shCSDE1) HEK293T cells transiently expressing FLAG-CSDE1. Data are presented as mean ± SD (**$P < 0.03$, $n = 3$, two-tailed t test). (**F**) Western blots confirming the ectopic expression of FLAG-tagged full length CSDE1 in CSDE1 knockdown (shCSDE1) HEK293T cells. β-Actin was used as a loading control.

at both mRNA and protein levels are enhanced in CSDE1 KO MEL cells relative to the Control (Figure 1F, G). We observed no changes in the expression of miRNA protein factors, namely, Drosha, DGCR8, Dicer and AGO2 in the absence of CSDE1 (Supplementary Figure S3), indicating that the effects of CSDE1 on miR-451 levels and target repression (Figure 1) are not a consequence of indirect effects due to changes in the expression of miRNA processing enzymes. Together, our results revealed that CSDE1 regulates the post-transcriptional accumulation of non-canonical mature miR-451.

CSDE1 promotes the processing of miR-451

To further investigate the role of CSDE1 in miR-451 biogenesis, we examined the expression pattern of miR-451 in CSDE1 KO erythroid cells. We observed that longer isoforms of mature miR-451 were accumulated relative to the Control cells while the expression of other miRNAs, for example, let-7 were unaltered (Figure 2A). Next, to identify the stage at which CSDE1 acts on miR-451, we transiently expressed miR-144/451 operon in HEK293T cells stably expressing shRNA targeting CSDE1 or a Control and measured the expression of miR-451. We observed accumulation of longer isoforms of mature miR-451, including the precursor in CSDE1 knockdown conditions, relative to the Control (Figure 2B, C). And vice versa, we observed a reduction in the expression of precursor miR-451 and an increase in the levels of mature miR-451 in shCSDE1 HEK293T cells transiently expressing FLAG-CSDE1 relative to the Vector Control (Figure 2D, F). Following, we evaluated the repression of miR-451 targets using luciferase reporter constructs and observed that the reintroduction of CSDE1 expression led to a decrease in the relative luciferase activity (Figure 2E, F). Collectively, these findings demonstrate that CSDE1 stimulates the processing of pre-miR-451.

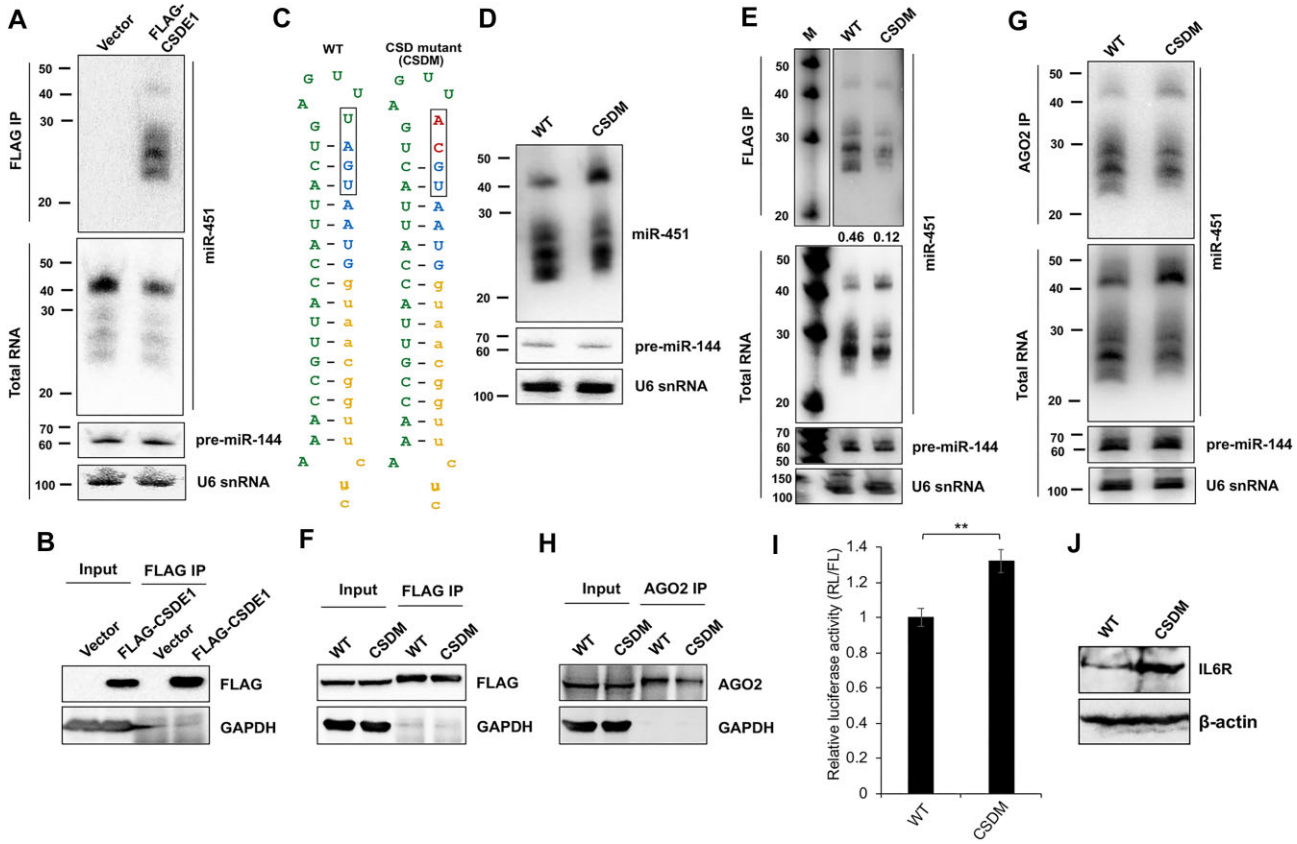

Figure 3. CSDE1 binds miR-451. (**A**) Northern blot analysis of miR-451 from immunoprecipitation of FLAG-CSDE1 and total RNA of Control and CSDE1 knockdown (shCSDE1) HEK293T cells transiently expressing miR-144/451 operon along with FLAG-CSDE1. (**B**) Western blot confirming the expression and immunoprecipitation efficiency of FLAG-CSDE1 from protein extracts under the aforementioned conditions. (**C**) pre-miR-451 hairpin with mutations in the CSD binding motif, UGAU. Green: mature miR-451, Blue: sequence trimmed by PARN. Yellow: sequence cleaved by AGO2. Nucleotides in red present mutations, 23U → A, 24A → C. (**D**) Northern blot analysis of miR-451 from total RNA of HEK293T cells transfected with plasmids expressing WT and CSDM pre-miR-451 along with FLAG-CSDE1. (**E**) Northern blot analysis of miR-451 from immunoprecipitation of FLAG-CSDE1 and total RNA of HEK293T cells transfected with plasmids expressing WT and CSDM pre-miR-451 along with FLAG-CSDE1. The quantification of miR-451 species (densitometry analysis of band intensity) in each lane of the FLAG IP relative to its corresponding lane in total RNA is presented underneath the blot. (**F**) Western blot confirming the expression and immunoprecipitation efficiency of FLAG-CSDE1 from protein extracts under the same conditions. (**G**) Northern blot analysis of miR-451 from immunoprecipitation of endogenous AGO2 and total RNA of HEK293T cells transfected with plasmids expressing WT and CSDM pre-miR-451. The RNA extracts were run on 8 M urea–PAGE gel, and the miRNAs indicated were probed. Migration of the molecular weight marker is indicated (nt). Pre-miR-144 was probed as a transfection control while U6 snRNA was used as a loading control. (**H**) Western blot confirming the expression and immunoprecipitation efficiency of AGO2 from protein extracts under the same conditions. GAPDH was used as a loading control. (**I**) Relative luciferase expression (renilla/ firefly) of miR-451 reporter construct in HEK293T cells transiently expressing the wild type pre-miR-451 and the CSD mutant pre-miR-451. Data are presented as mean ± SD (**$P < 0.03$, $n = 3$, two-tailed t test). (**J**) Western blot confirming the expression of IL6R in HEK293T cells transfected with the WT and CSDM pre-miR-451 constructs. β-Actin was used as a loading control.

CSDE1 binding is critical to the processing of pre-miR-451

Among proteins with Cold Shock Domains (CSD), Lin28 binds a four-nucleotide motif in pre-miRNAs, notably let-7 family and alters their processing into mature form (50). Since CSDE1 contains five canonical CSDs (51), initially we examined the expression and length distribution of let-7 family miRNAs, for instance let-7b-5p and let-7a-5p which consists of Lin28 CSD binding motif or not, respectively. As shown in Supplementary Figure S4, there was no change in their expression pattern under CSDE1 KO conditions (Supplemental File 3). Interestingly, the CSD binding motif, UGAU is present in miR-451 sequence and CSDE1 influences miR-451 expression. Therefore, we sought to investigate binding of miR-451 to CSDE1. Here, we transiently expressed the miR-144/451 operon in CSDE1 knocked down HEK293T cells and measured the expression of miR-451 in RNA extracts from immunoprecipitation of FLAG-CSDE1 and observed that CSDE1 binds both the precursor/intermediate and mature forms of miR-451 (Figure 3A, B). Next, we investigated whether UGAU, a sequence similar to Lin28 CSD binding motif (50), is responsible for CSDE1 association to miR-451. Based on the earlier systematic mutational analysis of individual nucleotide positions and base-pairing requirements in the pre-miR-451 stem and loop sequence within the context of a functional human pri-mir-144/mir-451 expression construct (52), we generated miR-144/451 plasmids with point mutations in the motif UGAU at positions 23U, 24A on miR-451 sequence (Figure 3C). Our expression analysis followed by immunoprecipitation of FLAG-CSDE1 revealed

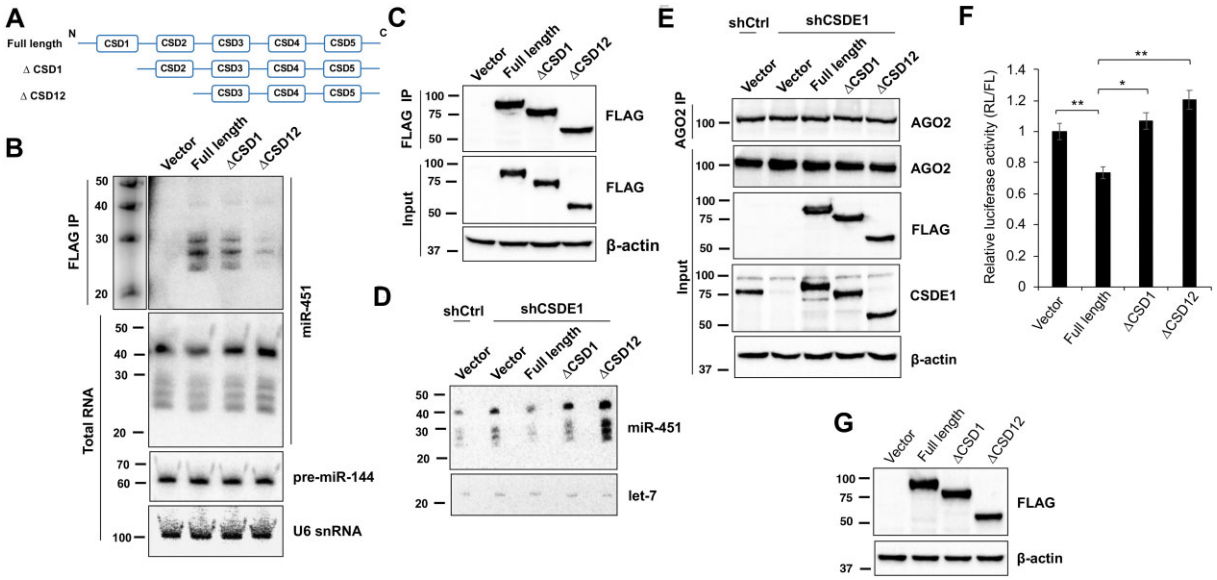

Figure 4. The N-terminal domains of CSDE1 influence miR-451 expression. (**A**) Schematics of the deletion mutants of CSDE1 used in the study. (B, D) Northern blot analysis of indicated miRNAs from immunoprecipitation of FLAG-CSDE1 and total RNA (**B**) as well as AGO2 IP (**D**) from CSDE1 knockdown (shCSDE1) HEK293T cells transiently expressing miR-144/451 operon along with FLAG-tagged full length and deletion mutants of CSDE1. The RNA extracts were run on the 8 M urea–PAGE gel, and the miRNAs indicated were probed. Migration of the molecular weight marker is indicated (nt). Pre-miR-144 was probed as a transfection control while U6 snRNA was used as a loading control. (**C**, **E**) Immunoprecipitation (IP) of FLAG-CSDE1 and AGO2 was performed under the same conditions. The immunoprecipitates were run on the SDS–PAGE gel and the proteins indicated were probed. (**F**) Relative luciferase levels (renilla/firefly) of miR-451 reporter construct in CSDE1 knockdown (shCSDE1) HEK293T cells transiently expressing FLAG-tagged full length and deletion mutants of CSDE1. Data are presented as mean ± SD (**$P < 0.03$; *$P < 0.05$; $n = 3$, two-tailed t test). (**G**) Representative figure for the western blot confirming the expression of FLAG-tagged CSDE1 and its mutants in CSDE1 knockdown (shCSDE1) HEK293T cells used for the luciferase assays. Migration of the molecular weight marker is indicated (kD). β-Actin was used as a loading control.

that CSDE1 binds less to the mutated miR-451 relative to the wild type (WT) (Figure 3D–F), indicating that the CSD binding motif UGAU is critical for CSDE1 association to miR-451. In addition, we observed that the mutations in the motif led to accumulation of miR-451 precursor bound to AGO2 which is consistent with its levels in total RNA (Figure 3G-H). Further, we evaluated the importance of CSD binding motif in the repression of miR-451 targets using luciferase reporter constructs. As shown in Figure 3I, the relative luciferase activity is higher in cells transfected with the CSD mutant (CSDM) of pre-miR-451 relative to the WT pre-miR-451. Consistent with the reduced target gene silencing evident from the reporter assays, we observed enhanced expression of miR-451 target IL6R in the case of CSD mutant, relative to the wild type pre-miR-451 (Figure 3J). Together, our results indicate that CSDE1 binding is critical to the biogenesis of miR-451.

The N-terminal domains of CSDE1 influence the processing of precursor miR-451

CSDE1 interacts with AGO2 through its N-terminal domains, especially CSD1 (35, Figure 5C). Thus, to investigate the role of cold shock domains 1 and 2 (depicted in pictorial representation, Figure 4A) in the processing of pre-miR-451, we transiently expressed CSDE1 deletion mutants, ΔCSD1 (that lost interaction with AGO2) and ΔCSD12 and measured the expression of miR-451. The expression of pre-miR-451 is higher in case of ΔCSD1 and ΔCSD12 relative to the full length CSDE1 in total RNA (Figure 4B, C) and the RNA extracts from AGO2 immunoprecipitation (Figure 4D, E). However, CSDE1 binding of miR-451 is significantly reduced among the deletion mutants ΔCSD1 and ΔCSD12 relative to the full length CSDE1 (Figure 4A, B). Next, to determine whether the domains responsible for CSDE1 interaction with AGO2 are necessary for miR-451 target repression, we transiently expressed the N-terminal FLAG-CSDE1 and its deletion mutants (ΔCSD1 and ΔCSD12) in CSDE1 depleted background and performed luciferase reporter assays for miR-451. As shown in Figure 4F, there was a significant difference in the luciferase activity in the presence of the deletion mutant ΔCSD12 when compared to either the full length CSDE1 or ΔCSD1 proteins. The expression of full length CSDE1 and its deletion mutants for the reporter assays were comparable, as presented in Figure 4G. As a whole, these results support that CSDE1 binding to both miR-451 and AGO2 is required for efficient processing of pre-miR-451.

CSDE1 interacts with the poly(A)-specific ribonuclease PARN

Poly(A)-specific ribonuclease (PARN) sculpts the 3′ ends of miRNAs in human cells and depletion of PARN leads to the accumulation of the 26 nt intermediate miR-451 (13,38). Since depletion of PARN leads to accumulation of miR-451 intermediates of 26 nt similar to that of CSDE1 (13,38) (Figure 1C, D), initially we juxtaposed the expression of miR-451 from PARN and CSDE1 KO cells. As shown in Supplementary Figure S5A, B, the longer isoforms of miR-451 were observed in CSDE1 KO cells similar

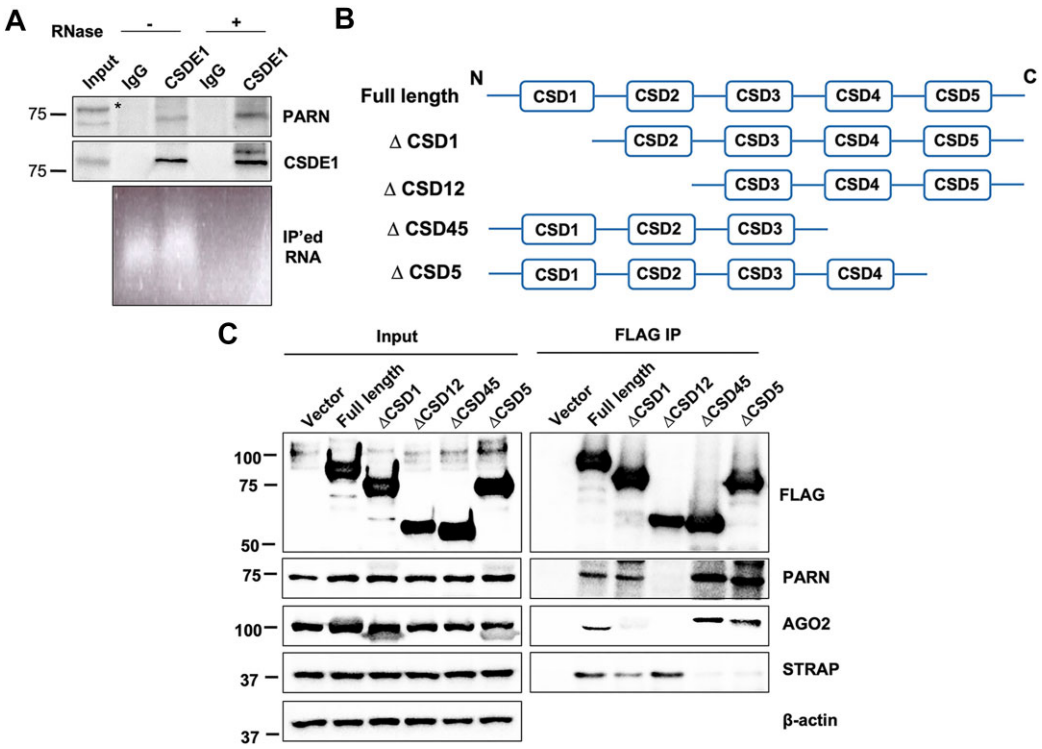

Figure 5. CSDE1 is associated with PARN. (**A**) Immunoprecipitation of endogenous CSDE1 using anti-CSDE1 antibody from the lysate of MEL cells, before (−) and after (+) RNases treatment. * Indicates non-specific bands. Agarose gel image of IP'ed RNA before (−) and after (+) RNases treatment is presented underneath the western blots. (**B**) Schematics of the deletion mutants of CSDE1 used in the study. (**C**) Immunoprecipitation (IP) of CSDE1 was performed using anti-FLAG antibody from the lysate of HEK293T cells transiently expressing FLAG-tagged full length and deletion mutants of CSDE1. The immunoprecipitates were run on the SDS–PAGE gel and the proteins indicated were probed. Migration of the molecular weight marker is indicated (kD).

to that of PARN KO. Next, as CSDE1 and PARN each interact with AGO2, we sought to investigate whether CSDE1 interacts with PARN. As shown in Figure 5A, CSDE1 interacts with PARN, and it is RNA-independent. Following, we examined AGO2 interaction with PARN in absence of CSDE1 and the findings suggest that AGO2 association with PARN is independent of CSDE1 (Supplementary Figure S5C). Later, to determine which of the CSD domains is responsible for CSDE1 interaction with PARN, the N-terminal FLAG-CSDE1 and its deletion mutants (ΔCSD1, ΔCSD12, ΔCSD45, ΔCSD5) (Figure 5B) were transiently expressed in HEK293T cells and immunoprecipitation was performed using FLAG antibody. We observed that the ΔCSD12 deletion mutant, but not ΔCSD1, lost the interaction with PARN, unlike AGO2 which binds CSDE1 via CSD1, while the C-terminal deletion mutants (ΔCSD45, ΔCSD5) retained interaction with both AGO2 and PARN (Figure 5C). Thus, our results indicate that CSD2 is accountable for interaction between CSDE1 and PARN.

CSDE1 regulates miR-451 trimming

To test whether CSDE1 is involved in the trimming of miR-451 intermediates, we performed trimming assays *in vitro* using synthetic intermediate miR-451 oligonucleotides, ac-pre-miR-451 (WT) (Figure 6A, left) incubated with cellular extracts of HEK293T cells under Control and CSDE1 KO conditions. We examined trimming efficiency at 48hrs, and interestingly, the probes were trimmed to below 26nt in length. Therefore, we measured the intensity of bands between 23nt and 26nt by densitometry analysis and their fraction in total are presented in the bar graph (Figure 6C, E). Of note, as miRNA trimming progresses, miRNA species of 23nt are generated more with a concomitant decrease in the miRNAs of 26nt (38). We observed that the proportion of the intensity of trimmed miR-451 at 23nt to 26nt is lower in the absence of CSDE1 relative to the Control, indicating CSDE1 positively regulates the trimming of intermediate pre-miR-451 *in vitro* (Figure 6B, C, Supplementary Figure S6A). Similarly, we investigated whether the CSD binding motif is required for trimming of the intermediate pre-miR-451. We used synthetic RNA oligonucleotides mutated for the CSDE1 binding (ac-pre-miR-451 CSDM), Figure 6A, right) and performed trimming assays. As shown in Figure 6D-E, Supplementary Figure S6B, processing of ac-pre-miR-451 CSDM accumulates miR-451 of 25nt in length and does not yield efficiently into mature miR-451 of 23nt, compared to the WT ac-pre-miR-451, indicating CSDE1 binding of the intermediate miR-451 is necessary for its trimming. Additionally, to delineate the possibility that mutation in CSD binding motif is too disruptive to the overall structure and may have resulted in indirect effects, we performed *in vitro* trimming assays using hairpin mimics, ac-pre-miR-451 WT and ac-pre-miR-451 Swapped Stem (Supplementary Figure S7A). Of note, we swapped the nucleotides in the terminal stem loop at posi-

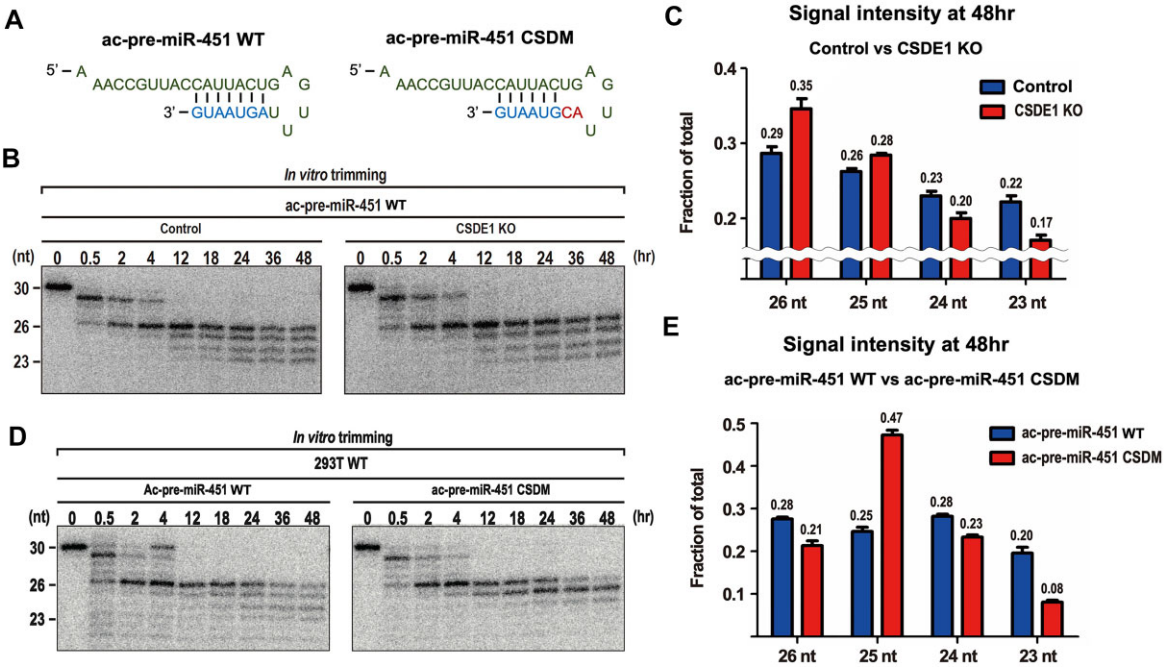

Figure 6. CSDE1 assists miR-451 trimming. (**A**) Sequence schematics of the synthetic intermediate RNA oligonucleotides of wild type pre-miR-451 (ac-pre-miR-451 WT, left) and its CSD binding mutant (ac-pre-miR-451 CSDM, right) used in the trimming assays *in vitro*. (**B**, **D**) The 5′ ends of respective RNA probes, ac-pre-miR-451 WT and ac-pre-miR-451 CSDM were labelled and incubated for the time periods indicated with cytoplasmic lysate transiently expressing FLAG- tagged AGO2 in Control and CSDE1 KO HEK293T cells (B) and the Control HEK293T cells only (D), respectively. The RNA extracts were resolved on urea–PAGE gels. C, E) Bar graph representation of band intensity of miR-451 of varying lengths at 48hr in Control versus CSDE1 KO HEK293T cell lysate supplied with the ac-pre-miR-451 WT (**C**) and HEK293T cells supplied with ac-pre-miR-451 WT and ac-pre-miR-451 CSDM (**E**). The upper number of each graph bar represents fraction of total.

tion 23 and 24, which effectively mutated the motif UGAU but still maintain the G:U wobble and likely to preserve stem loop structure similar to the WT precursor. We observed lower trimming, i.e. lower the ratio of band intensity corresponding to 23–21nt, indicative of mature miR-451, in the case of ac-pre-miR-451 Swapped Stem, compared to the WT (Supplementary Figure S7B-C). Collectively, these results demonstrate that CSDE1 assists in the trimming of intermediate miR-451.

DISCUSSION

The miRNA expression levels are governed by the processing efficiency of their precursors through Drosha and Dicer or AGO2. This efficiency can be determined either by structural and sequence features of miRNA precursors which directly affect the processing machinery, or by RBPs that recognize specific sequences within miRNA precursors and modulate their processing depending on the cellular context (1,53–54).

In the present study, we show that CSDE1 controls the expression of miR-451 in erythroleukemia cells (Figure 1–2). Although, other canonical miRNAs showed reduced expression in CSDE1 KO conditions, none of the candidates (except miR-451) presented significant variation in the distribution of sequence reads corresponding to both their mature and precursor forms (Figure 1C, D, Supplementary Figure S2). These observations once again highlight the atypical nature of miR-451 biogenesis and supports the unique role played by CSDE1 in controlling miR-451 expression. CSDE1 and miR-451 are highly abundant in erythrocytes (14–18,37). CSDE1 binds the CSD motif UGAU in pre-miR-451 and the loss of CSDE1 or its binding leads to the accumulation of pre-miR-451 (Figure 3). However, we observed no change in the expression of let-7b-5p, a member of let-7 family, which consists of the CSD binding motif. It is likely because the processing of let-7b-5p is dependent on Dicer unlike miR-451 which requires AGO2 catalytic activity. It is evident from our data that CSDE1 binding to pre-miR-451 and interaction with AGO2 facilitates the processing of the precursor into the mature form (Figure 4).

Of note, the lower pre-miR-451 levels in the RNA isolated from the immunoprecipitation of CSDE1 deletion mutants, i.e. ΔCSD1 and ΔCSD12, despite the corresponding accumulation of pre-miR-451 in the total RNA (Figure 4B) supports the importance of CSDE1 binding to pre-miR-451 for the efficient processing of miR-451 precursor. CSD1 and CSD2 are responsible for RNA binding ability of CSDE1 (24) and CSD1 is necessary for interaction of CSDE1 with AGO2 (35). Since ΔCSD12 (devoid of both CSD1 and CSD2) can no longer bind miR-451 species and the AGO2, it is likely that the miR-451 is not processed and therefore stuck in AGO2, as seen in higher band intensity of miR-451 species (Figure 4B, D). The loss of pre-miR-451 binding to the N-terminal deletion mutants reinforces the notion that CSDE1 N-terminal domains are critical for its post-transcriptional role in RNA metabolism. Additionally, the levels of pre-miR-451 bound to AGO2 were reduced in cells expressing the full length CSDE1 compared to the vector

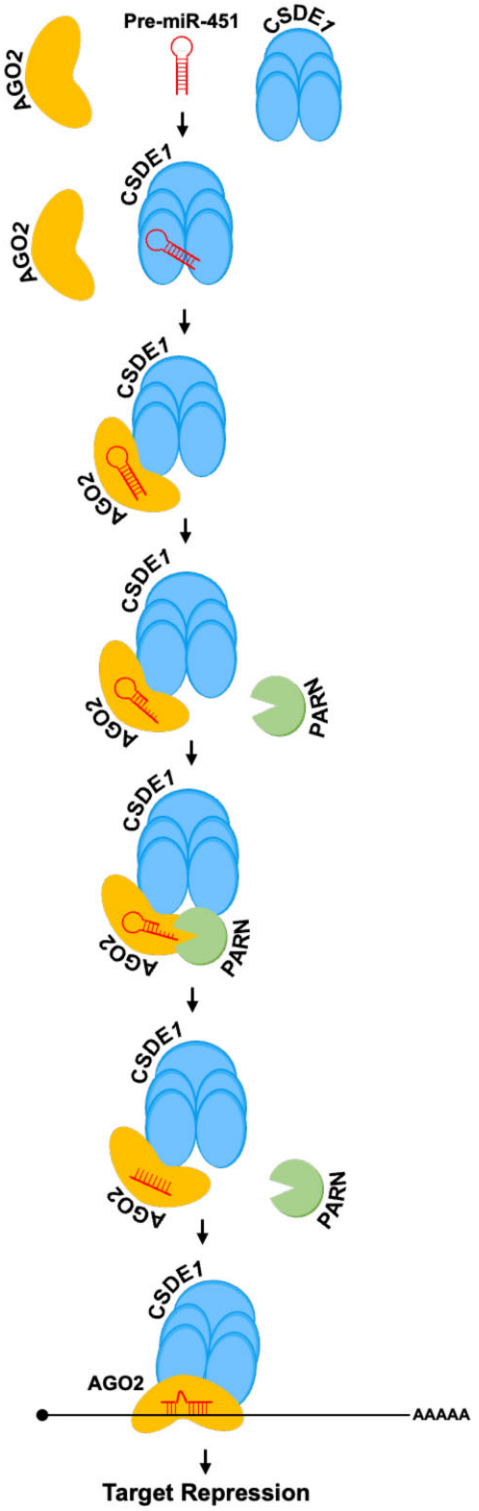

Figure 7. CSDE1 facilitates the biogenesis of miR-451. CSDE1 acts as a scaffold protein that binds pre-miR-451 and recruits AGO2 and PARN to process and generate mature miR-451 towards gene silencing.

control (Figure 4D). Since CSDE1 interacts with AGO2 within the miRISC and the mRNA decapping machinery to promote the silencing of targeted mRNAs (35, Figure 4F), it is possible that CSDE1 regulated processing of precursor and the generation of mature miR-451 becomes dynamic and rapid that led to recycling of AGO2 and therefore seen in terms of lower miR-451 species intensity bound to AGO2 under full length CSDE1 expression. Further, the band intensity of miR-451 species observed in the case of ΔCSD1 points to the possibility of a dynamic exchange of miR-451 between CSDE1 and AGO2, i.e. ΔCSD1 retains binding of miR-451 species and acts as a reservoir (Figure 4B) in the absence of AGO2 interaction or depending on the rate of recycling and availability of AGO2, for miR-451 processing and target gene silencing. This unique relation between CSDE1 and miR-451/AGO2 highlights the importance of RBPs in regulating cellular repertoire of distinct miRNA species depending on the context. It is in line with earlier studies that demonstrate RBP binding to pri/pre-miRNAs, for instance, in glioblastoma multiforme, the cold shock protein YBX-1 binds to the motif AACAUC in the terminal loop region of pri-/pre-miR-29b-2 and regulates the biogenesis of mature miR-29b-2 (1,55). Interestingly, CSDE1 acts as a tumor suppressor or an oncogene depending on the cellular context and both CSDE1 and miR-451 are required for the differentiation of erythroblasts into mature red blood cells, the process which becomes subverted in erythroleukemia (22,36–37). Therefore, it would be interesting for future studies to focus on the mutational landscape of pre-miR-451, especially in CSD binding motif, in the genetic background of leukemia patients and investigate how such genetic variants influence the pathological outcomes of blood cancers.

CSDE1 interacts with PARN via its N-terminal domain CSD2 and assists in the trimming of intermediate miR-451 through its CSD binding motif (Figure 5–6, Supplementary Figure S5-S7). The accumulation of intermediate miR-451 along with pre-miR-451 in the RNA samples from AGO2 immunoprecipitation under ΔCSD12 conditions in comparison to ΔCSD1 (Figure 4D) reveals the functional importance of CSDE1 interaction with PARN (via CSD2) in addition to AGO2 (via CSD1) for effective processing of miR-451. Earlier studies have shown that trimming of miR-451 is dispensable for target silencing *in vitro* and in cultured cells (13). However, recent studies demonstrated that the non-canonical binding sites in the 3′ end of the miRNA (beyond the seed region) determine the specificity and efficiency of target mRNA repression (56–57). Therefore, it would be exciting for future studies to focus on the target repertoire of miR-451 in erythroleukemia cells that are dependent on CSDE1 mediated trimming of the intermediate into the mature length which may facilitate binding to specific mRNAs underlying erythrocyte differentiation *in vivo.*

Overall, the mechanistic details elucidated in the present study demonstrate a new role for CSDE1 as a scaffold protein that binds pre-miR-451 and recruits AGO2 and PARN to efficiently process and generate mature miR-451 towards specific gene silencing in erythroid progenitor cells (Figure 7). Having already elucidated the involvement of CSDE1 in miRNA-guided translational control and/or mRNA decay (35–36), the current findings highlight the importance

of feedback loop or coupling of miRNA biogenesis with specific silencing of target mRNAs bound by RBPs. This is in line with earlier reports on eIF1A which interacts with AGO2 and augments its function in the processing of miR-451 and translational repression of its targets towards erythrocyte maturation in zebrafish (58). Additionally, the distinct allocation of CSDE1 domains for its association with AGO2 (via CSD1) and PARN (via CSD2) points to the dynamics of protein complexes associated with pre-miR-451 processing to generate a functional miRISC towards efficient silencing of target genes underlying erythropoiesis. We believe that findings from our study will open new avenues of study on the regulatory role of CSDE1 in the miRNA-driven pathology of blood cancers which could inform the design of therapeutic strategies to alleviate the blockage of erythroblast differentiation in leukemia treatment.

DATA AVAILABILITY

The BioProject accession number for the sequence data reported in this paper is PRJNA875097.

SUPPLEMENTARY DATA

Supplementary Data are available at NAR Online.

ACKNOWLEDGEMENTS

We thank all members of our laboratory for helpful discussions and grateful to Prof. Marieke von Lindern, Sanquin Research, Amsterdam for the generous gift of MEL Control and CSDE1 KO cell lines. We appreciate the support from Dr Gunter Meister and Dr Eric Lai for sharing of reagents and plasmids used in the study.

FUNDING

The Dean of Science Startup Funds, Memorial University of Newfoundland and Discovery Grant [RGPIN-2022-03780] from Natural Sciences and Engineering Research Council of Canada (to P.K.K.); Canadian Institutes of Health Research (CIHR) project grant (to M.J.S.); National Research Foundation of Korea (NRF) grant funded by the Ministry of Science and ICT (MSIT), Republic of Korea [NRF-2021R1A5A1032428, NRF-2022R1A2C1011032 to C.S.]; The New Breeding Technologies Development Program [RS-2022-RD009544]; Rural Development Administration Republic of Korea (to C.S.); P.K.K. and L.M.H. were recipients of scholarship from the Fonds de Recherche du Québec-Santé (FRQ-S).
Conflict of interest statement. None declared.

REFERENCES

1. Treiber,T., Treiber,N. and Meister,G. (2019) Regulation of microRNA biogenesis and its crosstalk with other cellular pathways. *Nat. Rev. Mol. Cell Biol.*, **20**, 5–20.
2. Bartel,D.P. (2018) Metazoan MicroRNAs. *Cell*, **173**, 20–51.
3. Berezikov,E., Chung,W.J., Willis,J., Cuppen,E. and Lai,E.C. (2007) Mammalian mirtron genes. *Mol. Cell*, **28**, 328–336.
4. Okamura,K., Hagen,J.W., Duan,H., Tyler,D.M. and Lai,E.C. (2007) The mirtron pathway generates microRNA-class regulatory RNAs in *Drosophila*. *Cell*, **130**, 89–100.
5. Ruby,J.G., Jan,C.H. and Bartel,D.P. (2007) Intronic microRNA precursors that bypass Drosha processing. *Nature*, **448**, 83–86.
6. Haussecker,D., Huang,Y., Lau,A., Parameswaran,P., Fire,A.Z. and Kay,M.A. (2010) Human tRNA-derived small RNAs in the global regulation of RNA silencing. *RNA*, **16**, 673–695.
7. Ender,C., Krek,A., Friedlander,M.R., Beitzinger,M., Weinmann,L., Chen,W., Pfeffer,S., Rajewsky,N. and Meister,G. (2008) A human snoRNA with microRNA-like functions. *Mol. Cell*, **32**, 519–528.
8. Xie,M., Li,M., Vilborg,A., Lee,N., Shu,M.D., Yartseva,V., Sestan,N. and Steitz,J.A. (2013) Mammalian 5'-capped microRNA precursors that generate a single microRNA. *Cell*, **155**, 1568–1580.
9. Cheloufi,S., Dos Santos,C.O., Chong,M.M. and Hannon,G.J. (2010) A dicer-independent miRNA biogenesis pathway that requires Ago catalysis. *Nature*, **465**, 584–589.
10. Cifuentes,D., Xue,H., Taylor,D.W., Patnode,H., Mishima,Y., Cheloufi,S., Ma,E., Mane,S., Hannon,G.J., Lawson,N.D. *et al.* (2010) A novel miRNA processing pathway independent of Dicer requires Argonaute2 catalytic activity. *Science*, **328**, 1694–1698.
11. Yang,J.S. and Lai,E.C. (2010) Dicer-independent, Ago2-mediated microRNA biogenesis in vertebrates. *Cell Cycle*, **9**, 4455–4460.
12. Yang,J.S., Maurin,T., Robine,N., Rasmussen,K.D., Jeffrey,K.L., Chandwani,R., Papapetrou,E.P., Sadelain,M., O'Carroll,D. and Lai,E.C. (2010) Conserved vertebrate mir-451 provides a platform for Dicer-independent, Ago2-mediated microRNA biogenesis. *Proc. Natl. Acad. Sci. USA*, **107**, 15163–15168.
13. Yoda,M., Cifuentes,D., Izumi,N., Sakaguchi,Y., Suzuki,T., Giraldez,A.J. and Tomari,Y. (2013) Poly(A)-specific ribonuclease mediates 3'-end trimming of Argonaute2-cleaved precursor microRNAs. *Cell Rep.*, **5**, 715–726.
14. Pase,L., Layton,J.E., Kloosterman,W.P., Carradice,D., Waterhouse,P.M. and Lieschke,G.J. (2009) miR-451 regulates zebrafish erythroid maturation *in vivo* via its target gata2. *Blood*, **113**, 1794–1804.
15. Rasmussen,K.D., Simmini,S., Abreu-Goodger,C., Bartonicek,N., Di Giacomo,M., Bilbao-Cortes,D., Horos,R., Von Lindern,M., Enright,A.J. and O'Carroll,D. (2010) The miR-144/451 locus is required for erythroid homeostasis. *J. Exp. Med.*, **207**, 1351–1358.
16. Zhan,M., Miller,C.P., Papayannopoulou,T., Stamatoyannopoulos,G. and Song,C.Z. (2007) MicroRNA expression dynamics during murine and human erythroid differentiation. *Exp. Hematol.*, **35**, 1015–1025.
17. Zhang,L., Flygare,J., Wong,P., Lim,B. and Lodish,H.F. (2011) miR-191 regulates mouse erythroblast enucleation by down-regulating Riok3 and Mxi1. *Genes Dev.*, **25**, 119–124.
18. Patrick,D.M., Zhang,C.C., Tao,Y., Yao,H., Qi,X., Schwartz,R.J., Jun-Shen Huang,L. and Olson,E.N. (2010) Defective erythroid differentiation in miR- 451 mutant mice mediated by 14-3-3zeta. *Genes Dev.*, **24**, 1614–1619.
19. Yu,D., dos Santos,C.O., Zhao,G., Jiang,J., Amigo,J.D., Khandros,E., Dore,L.C., Yao,Y., D'Souza,J., Zhang,Z. *et al.* (2010) miR-451 protects against erythroid oxidant stress by repressing 14-3-3zeta. *Genes Dev.*, **24**, 1620–1633.
20. Bruchova,H., Yoon,D., Agarwal,A.M., Mendell,J. and Prchal,J.T. (2007) Regulated expression of microRNAs in normal and polycythemia vera erythropoiesis. *Exp. Hematol.*, **35**, 1657–1667.
21. Bruchova,H., Merkerova,M. and Prchal,J.T. (2008) Aberrant expression of microRNA in polycythemia vera. *Haematologica*, **93**, 1009–1016.
22. Kretov,D.A., Walawalkar,I.A., Mora-Martin,A., Shafik,A.M., Moxon,S. and Cifuentes,D. (2020) Ago2-dependent processing allows miR-451 to evade the global MicroRNA turnover elicited during erythropoiesis. *Mol. Cell.*, **78**, 317–328.
23. Mihailovich,M., Militti,C., Gabaldón,T. and Gebauer,F. (2010) Eukaryotic cold shock domain proteins: highly versatile regulators of gene expression. *Bioessays*, **32**, 109–118.
24. Hollmann,N.M., Jagtap,P.K.A., Masiewicz,P., Guitart,T., Simon,B., Provaznik,J., Stein,F., Haberkant,P., Sweetapple,L.J., Villacorta,L. *et al.* (2020) Pseudo-RNA-binding domains mediate RNA structure specificity in upstream of N-Ras. *Cell Rep.*, **32**, 107930.
25. Abaza,I., Coll,O., Patalano,S. and Gebauer,F. (2006) *Drosophila* UNR is required for translational repression of male-specific lethal 2 mRNA during regulation of X-chromosome dosage compensation. *Genes Dev.*, **20**, 380–389.
26. Duncan,K., Grskovic,M., Strein,C., Beckmann,K., Niggeweg,R., Abaza,I., Gebauer,F., Wilm,M. and Hentze,M.W. (2006) Sex-lethal

imparts a sex-specific function to UNR by recruiting it to the msl-2 mRNA 3′ UTR: translational repression for dosage compensation. *Genes Dev.*, **20**, 368–379.
27. Dormoy-Raclet,V., Markovits,J., Jacquemin-Sablon,A. and Jacquemin-Sablon,H. (2005) Regulation of Unr expression by 5′- and 3′-untranslated regions of its mRNA through modulation of stability and IRES mediated translation. *RNA Biol.*, **2**, e27–e35.
28. Schepens,B., Tinton,S.A., Bruynooghe,Y., Parthoens,E., Haegman,M., Beyaert,R. and Cornelis,S. (2007) A role for hnRNP C1/C2 and Unr in internal initiation of translation during mitosis. *EMBO J.*, **26**, 158–169.
29. Mitchell,S.A., Brown,E.C., Coldwell,M.J., Jackson,R.J. and Willis,A.E. (2001) Protein factor requirements of the Apaf-1 internal ribosome entry segment: roles of polypyrimidine tract binding protein and upstream of N-ras. *Mol. Cell Biol.*, **21**, 3364–3374.
30. Cornelis,S., Tinton,S.A., Schepens,B., Bruynooghe,Y. and Beyaert,R. (2005) UNR translation can be driven by an IRES element that is negatively regulated by polypyrimidine tract binding protein. *Nucleic Acids Res.*, **33**, 3095–3108.
31. Dinur,M., Kilav,R., Sela-Brown,A., Jacquemin-Sablon,H. and Naveh-Many,T. (2006) *In vitro* evidence that upstream of N-ras participates in the regulation of parathyroid hormone messenger ribonucleic acid stability. *Mol. Endocrinol.*, **20**, 1652–1660.
32. Lee,H.J., Bartsch,D., Xiao,C., Guerrero,S., Ahuja,G., Schindler,C., Moresco,J.J., Yates 3rd,J.R., Gebauer,F., Bazzi,H. *et al.* (2017) A post-transcriptional program coordinated by CSDE1 prevents intrinsic neural differentiation of human embryonic stem cells. *Nat. Commun.*, **8**, 1456.
33. Elatmani,H., Dormoy-Raclet,V., Dubus,P., Dautry,F., Chazaud,C. and Jacquemin-Sablon,H. (2011) The RNA-binding protein Unr prevents mouse embryonic stem cells differentiation toward the primitive endoderm lineage. *Stem Cell Rep.*, **29**, 1504–1516.
34. Wurth,L., Papasaikas,P., Olmeda,D., Bley,N., Calvo,G.T., Guerrero,S., Cerezo-Wallis,D., Martinez-Useros,J., García-Fernández,M., Hüttelmaier,S. *et al.* (2016) UNR/CSDE1 drives a post-transcriptional program to promote melanoma invasion and metastasis. *Cancer Cell*, **30**, 694–707.
35. Kakumani,P.K., Harvey,L.M., Houle,F., Guitart,T., Gebauer,F. and Simard,M.J. (2020) CSDE1 controls gene expression through the miRNA-mediated decay machinery. *Life Sci. Alliance*, **3**, e201900632.
36. Kakumani,P.K., Guitart,T., Houle,F., Harvey,L.M., Goyer,B., Germain,L., Gebauer,F. and Simard,M.J. (2021) CSDE1 attenuates microRNA-mediated silencing of PMEPA1 in melanoma. *Oncogene*, **40**, 3231–3244.
37. Horos,R., Ijspeert,H., Pospisilova,D., Sendtner,R., Andrieu-Soler,C., Taskesen,E., Nieradka,A., Cmejla,R., Sendtner,M., Touw,I.P. *et al.* (2012) Ribosomal deficiencies in Diamond-Blackfan anemia impair translation of transcripts essential for differentiation of murine and human erythroblasts. *Blood*, **119**, 262–272.
38. Lee,D., Park,D., Park,J.H., Kim,J.H. and Shin,C. (2019) Poly(A)-specific ribonuclease sculpts the 3' ends of microRNAs. *RNA*, **25**, 388–405.
39. Park,J.H., Shin,S.Y. and Shin,C. (2017) Non-canonical targets destabilize microRNAs in human Argonautes. *Nucleic Acids Res.*, **45**, 1569–1583.
40. Jee,D., Yang,J.S., Park,S.M., Farmer,D.T., Wen,J., Chou,T., Chow,A., McManus,M.T., Kharas,M.G. and Lai,E.C. (2018) Dual strategies for argonaute2-mediated biogenesis of erythroid miRNAs underlie conserved requirements for slicing in mammals. *Mol. Cell*, **69**, 265–278.
41. Li,L., Dai,H., Nguyen,A.P. and Gu,W. (2020) A convenient strategy to clone small RNA and mRNA for high throughput sequencing. *RNA*, **26**, 218–227.
42. Shrinet,J., Nandal,U.K., Adak,T., Bhatnagar,R.K. and Sunil,S. (2014) Inference of the oxidative stress network in Anopheles stephensi upon Plasmodium infection. *PLoS One*, **9**, e114461.
43. Krueger,F. (2015) Trim galore: a wrapper tool around Cutadapt and FastQC to consistently apply quality and adapter trimming to FastQ files. **516**517.
44. Kozomara,A., Birgaoanu,M. and Griffiths-Jones,S. (2019) miRbase: from microRNA sequences to function. *Nucleic Acids Res.*, **47**, D155–D162.
45. Griffiths-Jones,S., Saini,H.K., Van Dongen,S. and Enright,A.J. (2007) miRbase: tools for microRNA genomics. *Nucleic Acids Res.*, **36**, D154–D158.
46. Langmead,B., Trapnell,C., Pop,M. and Salzberg,S.L. (2009) Ultrafast and memory-efficient alignment of short DNA sequences to the human genome. *Genome Biol.*, **10**, R25.
47. Bossé,G.D., Rüegger,S., Ow,M.C., Vasquez-Rifo,A., Rondeau,E.L., Ambros,V.R., Grosshans,H. and Simard,M.J. (2013) The decapping scavenger enzyme DCS-1 controls microRNA levels in Caenorhabditis elegans. *Mol. Cell*, **50**, 281–287.
48. Moore,K.S., Yagci,N., Alphen,F.V., Paolini,N.A., Horos,R., Held,N.M., Houtkooper,R.H., Akker,E.V.D., Meijer,A.B., Hoen,P.A.C. *et al.* (2018) Csde1 binds transcripts involved in protein homeostasis and controls their expression in an erythroid cell line. *Sci. Rep.*, **8**, 2628.
49. Huang,H.Y., Lin,Y.C., Cui,S., Huang,Y., Tang,Y., Xu,J., Bao,J., Li,Y., Wen,J., Zuo,H. *et al.* (2022) miRTarBase update 2022: an informative resource for experimentally validated miRNA-target interactions. *Nucleic Acids Res.*, **50**, D222–D230.
50. Ustianenko,D., Chiu,H.S., Treiber,T., Weyn-Vanhentenryck,S.M., Treiber,N., Meister,G., Sumazin,P. and Zhang,C. (2018) LIN28 selectively modulates a subclass of Let-7 MicroRNAs. *Mol. Cell*, **71**, 271–283.
51. Hollmann,N.M., Jagtap,P.K.A., Masiewicz,P., Guitart,T., Simon,B., Provaznik,J., Stein,F., Haberkant,P., Sweetapple,L.J., Villacorta,L. *et al.* (2020) Pseudo-RNA-binding domains mediate RNA structure specificity in upstream of N-Ras. *Cell Rep.*, **32**, 107930.
52. Yang,J.S., Maurin,T. and Lai,E.C. (2012) Functional parameters of Dicer-independent microRNA biogenesis. *RNA*, **18**, 945–957.
53. Auyeung,V.C., Ulitsky,I., McGeary,S.E. and Bartel,D.P. (2013) Beyond secondary structure: primary-sequence determinants license pri-miRNA hairpins for processing. *Cell*, **152**, 844–858.
54. Treiber,T., Treiber,N., Plessmann,U., Harlander,S., Daiß,J.L., Eichner,N., Lehmann,G., Schall,K., Urlaub,H. and Meister,G. (2017) A compendium of RNA-binding proteins that regulate MicroRNA biogenesis. *Mol. Cell*, **66**, 270–284.
55. Wu,S.L., Fu,X., Huang,J., Jia,T.T., Zong,F.Y., Mu,S.R., Zhu,H., Yan,T., Qiu,S., Wu,Q. *et al.* (2015) Genome-wide analysis of YB-1-RNA interactions reveals a novel role of YB-1 in miRNA processing in glioblastoma multiforme. *Nucleic Acids Res.*, **43**, 8516–8528.
56. Broughton,J.P., Lovci,M.T., Huang,J.L., Yeo,G.W. and Pasquinelli,A.E. (2016) Pairing beyond the Seed Supports MicroRNA Targeting Specificity. *Mol. Cell*, **64**, 320–333.
57. McGeary,S.E., Bisaria,N., Pham,T.M., Wang,P.Y. and Bartel,D.P. (2022) MicroRNA 3'-compensatory pairing occurs through two binding modes, with affinity shaped by nucleotide identity and position. *Elife*, **11**, e69803.
58. Yi,T., Arthanari,H., Akabayov,B., Song,H., Papadopoulos,E., Qi,H.H., Jedrychowski,M., Güttler,T., Guo,C., Luna,R.E. *et al.* (2015) eIF1A augments Ago2-mediated Dicer-independent miRNA biogenesis and RNA interference. *Nat. Commun.*, **6**, 7194.